Preparation of clay/epoxy nanocomposites by layered-double-hydroxide initiated self-polymerization

Ying-Nan Chan [a], Tzong-Yuan Juang [a], Yi-Lin Liao [b], Shenghong A. Dai [a], Jiang-Jen Lin [b],*

[a] Department of Chemical Engineering, National Chung-Hsing University, Taichung, Taiwan
[b] Institute of Polymer Science and Engineering, National Taiwan University, Taipei, Taiwan

ABSTRACT

An anionic clay, magnesium–aluminum layered double hydroxide ($Mg_2Al–NO_3–LDH$), was prepared by a co-precipitation method and intercalated with poly(oxypropylene)–amindocarboxylic acid (POP–amido acid). Depending on the POP-intercalating agents with molecular weight at 2000 or 400 g/mol, the intercalated LDHs were analyzed to have *d* spacing of 6.8 or 2.7 nm and organic incorporation of 80 and 55 wt%, respectively. Two comparative POP/LDH hybrids were allowed to initiate the self-polymerization of the epoxy resin, diglycidyl ether of bisphenol-A (DGEBA). The curing rate was significantly increased by using the hybrids as initiators for epoxy curing, demonstrated by DSC thermal analysis that the exothermic peak shifted from 182 to 152 °C by increasing organoclay addition. The resultant nanocomposites prepared from the anionic LDH initiated epoxy self-polymerization have the improved thermal and physical properties, evidenced by TGA, XRD, TEM, and SEM analyses.

© 2008 Elsevier Ltd. All rights reserved.

1. Introduction

The polymer/clay nanocomposites have been intensively studied [1–10] since the first disclosure of the nylon-6/montmorillonite system by the Toyota Research Group [4,5]. The nanocomposites with fine dispersion of silicate platelets in the matrices may gain the enhanced property such as coefficients of expansion, flammability resistance [6,11–14], mechanical properties [15,16], and glass transition temperature [17–19]. The synthesis generally involves a complicated mixing process such as melt blending, solution blending, and in situ polymerization [20,21]. Hence, to develop a simple method for achieving a homogeneous distribution of randomized clays in polymer matrices is still a challenging task [10]. For most industrial practices, the epoxy resin of DGEBA may undergo two-component polymerization with a suitable curing agent [22,23], such as amines, phenols, anhydride, and cationic photoinitiators. Among the literature regarding to epoxies and their curing conditions, self-polymerization of epoxy ring-opening process is seldom reported [24–29]. Besides the uses of organic catalyst [24,25], it has been revealed that the organoclays derived from montmorillonite clay could be served as the initiator for the epoxy self-polymerization [26–29] and lowering the process activation energy, but ultimately forming a powder material that had no mechanical properties.

In our earlier works [30–32], we demonstrated the uses of organoclays for the synthesis of two-component epoxies. The organic modification to layered silicate clays is generally required for enhancing their compatibility with polymers. In the pursuit of clay-exfoliated nanocomposites for superior properties [30], we disclosed the new organic intercalating agents including hydrophobic poly(oxyalkylene)–diamine salts to expand the *d* spacing as high as 9.2 nm [33–36]. In addition, we explored the anionic LDH that was prepared from the intercalation with poly(oxyalkylene)–amido acids [37]. The intercalation afforded a series of different POP-embedded anionic clays, which can be employed for one-component epoxy self-polymerization as in the cationic MMT clays [38]. Herein, we reveal a facile preparation of LDH/epoxy nanocomposites, with two representative examples of POPs, POP2000–2MA/LDH (2000 g/mol molecular weight of POP and clay *d* spacing of 6.8 nm) and POP400–3MA/LDH (400 g/mol and 2.7 nm). With the optimized curing conditions and the choice of POP agents, fine dispersion of clay platelets in epoxy matrices has been achieved and characterized by using transmission electron microscope (TEM).

2. Experimental

2.1. Preparation of POP–amido acids

The poly(oxypropylene)–amines (POP–amines), including a diamine of 2000 g/mol M_w (POP2000), and a triamine of 400 g/mol M_w (POP400), were obtained from Huntsman Chemical Co. Maleic anhydride (MA) was purchased from Aldrich Chemical

* Corresponding author. Tel.: +886 2 3366 5312; fax: +886 2 3366 5237.
E-mail address: jianglin@ntu.edu.tw (J.-J. Lin).

Co., and purified by sublimation. The detailed procedures for preparing the POP–amido acids were reported previously [37]. Typically, the experiments were carried out in glassware reactor equipped with a mechanical stirrer and nitrogen inlet–outlet lines. The reactor was first charged with a designated amount of POP–amines dissolved in THF solvent followed by adding the stoichiometric amount of MA at ambient temperature. The reaction of 1:1 anhydride/amine molar ratio ($MA/NH_2 = 1/1$) afforded the products of POP–amido acids, POP2000–2MA for the diamine and POP400–3MA for the triamine adducts, with the chemical structures illustrated in Fig. 1. The epoxy resin, liquid form of diglycidyl ether of bisphenol-A (DGEBA, trade name BE-188, epoxide equivalent weight at 188), was obtained from Chang Chun Chemical Co., (Taiwan).

2.2. Preparation of POP–amido acid/LDH

$Mg_2Al–NO_3$–LDH was prepared by a co-precipitation process according to the procedures reported previously [39]. An example of ionic exchanging procedure for preparing POP2000–2MA intercalated LDH is described below. A portion of LDH (3.0 g) was placed in a 500 mL glassware reactor under nitrogen blanket and stirred vigorously in 200 mL deionized water at 80 °C. The slurry was poured with the solution of the POP2000–2MA sodium salts (13.2 g, 6 mmol), which was separately prepared by neutralizing the POP–amido acid with an equivalent amount of 2 N NaOH (6.0 g, 12 mmol) in 100 mL H_2O. The mixture was then stirred for 4 h and allowed to cool to ambient temperature. Similarly, the procedures were used for preparing POP400–3MA intercalated LDH. The XRD analyses exhibited d spacing of 6.8 and 2.7 nm and by TGA analyses the organic weight fraction was found to be 80/20 and 55/45 for the POP2000–2MA/LDH and POP400–3MA/LDH, respectively.

2.3. Preparation of POP–amido acid/LDH epoxy networks

The POP–amido acid/LDH epoxy networks were prepared by using various amounts of POP–amido acid/LDH as initiators (in epoxy resin with 5, 10, and 15 wt% of LDH). For example, POP2000–2MA/LDH (0.25 g) was dispersed in toluene (10 mL) at room temperature and mechanically stirred for 1 h followed by the epoxy resin (0.75 g) addition. After a thorough mixing, the viscous mixtures were poured into a flat aluminum-foil mould, and heated in a vacuum oven at temperatures of 120 °C for 1 h, 150 °C for 2 h, and 180 °C for 2 h. A sample plaque of cured epoxy product with 5 wt% clay content was obtained and named as 5 wt% POP2000–2MA/LDH epoxy network. A similar procedure was used to prepare POP400–3MA/LDH epoxy network and a control experiment of POP2000–2MA epoxy network without the LDH clay component.

2.4. Measurements

X-ray diffraction (XRD) was recorded on a Shimadzu SD-D1 diffractometer with a Cu target ($k = 1.5405$ Å). The d spacing of the epoxy nanocomposites was analyzed by using Bragg's equation ($n\lambda = 2d \sin \theta$). Thermal gravimetric analysis (TGA) was performed on a Seiko SII model SSC/5200, by heating the samples from 50 to 850 °C at a rate of 10 °C/min in air. Differential scanning calorimetry (DSC) was performed on a Perkin–Elmer DSC 7, at a heating scan of 10 °C/min. Scanning electron microscopy (SEM) was performed on a Topcon SEM (model: ABT-150a) to examine the fracture surfaces of the epoxy samples. Transmission electron microscopy (TEM) was performed on a Zeiss EM 902A at an acceleration voltage of 80 kV, and the samples with a thickness of approximately 80 nm were microtomed at room temperature using a diamond knife on a Reichert-Jung Ultracut UCT and transferred to carbon-film-coated Cu grids.

3. Results and discussion

3.1. POP–amido acid/LDH initiated epoxy self-polymerization

The curing profile of epoxy self-polymerization has been monitored through DSC thermal analysis by examining their curing
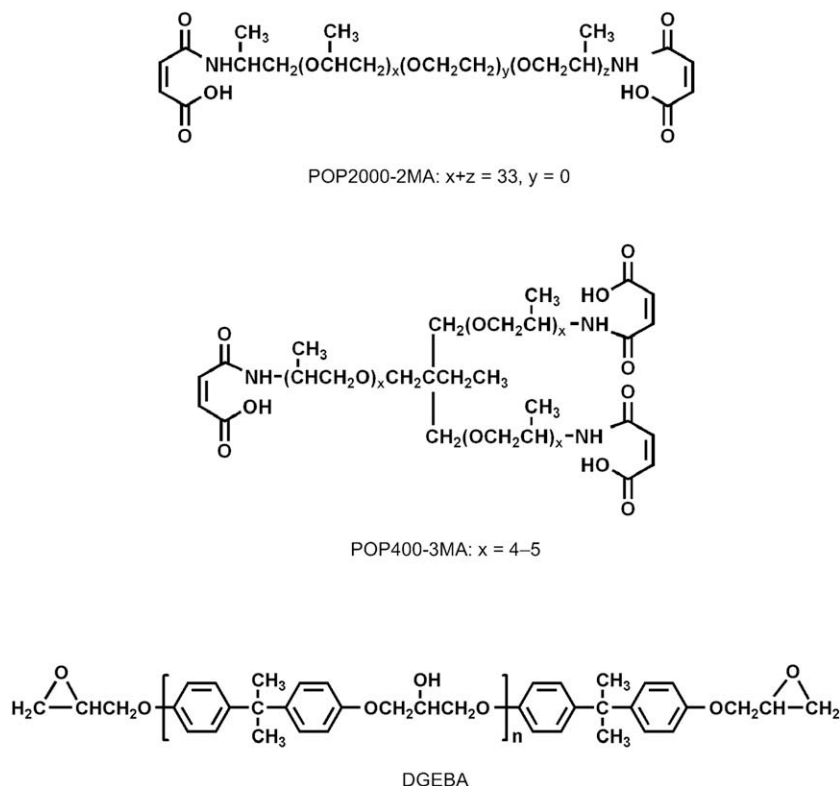

POP2000-2MA: x+z = 33, y = 0

POP400-3MA: x = 4–5

DGEBA

Fig. 1. Chemical structure of POP–amido acids and DGEBA epoxy resin.

exothermic peaks. As shown in Fig. 2, the epoxy polymerization initiated by POP2000–2MA, its sodium salts, and POP2000–2MA/LDH is exothermic during the epoxy ring-opening reaction. It was found that the POP2000–2MA could initiate the epoxy polymerization but giving rise to a set of two exothermic peaks at 136 and 194 °C (Fig. 2a), presumably caused by curing with different functionalities in POP–MA, such as carboxyl (–COO⁻H⁺) and amide groups (–CONH–) [40]. Similarly, the sodium salt of POP2000–2MA initiated the epoxy reaction with two exothermic peaks at 182 and 202 °C (Fig. 2b). However, with the POP-intercalated LDH as the initiator, the curing profile was substantially affected by the presence of the LDH clay. The catalytic effect of LDH is established by monitoring DSC exothermic temperatures with different LDH loadings. In the presence of 5–15 wt% of LDH, the polymerization produced only one exothermic DSC peak. With an increasing loading of POP2000–2MA/LDH, a lower exothermic temperature in the range of 152–182 °C was observed. Presumably, the epoxy monomers were able to migrate into the LDH clay galleries and initiated by the LDH surface ionic sites for the self-polymerization. The low curing temperature at 152 °C may be explained by the catalytic effect of LDH. Ultimately, the self-polymerization afforded the epoxy nanocomposites with the clay interlayer space to be widened or exfoliated in the polymer matrix.

3.2. Characterization of POP–amido acid/LDH epoxy networks

On the basis of XRD measurements, the pristine LDH clay has a d spacing of 0.78 nm in comparison with the POP–amido acid intercalated LDH, POP2000–2MA/LDH at 6.8 nm and POP400–3MA/LDH at 2.7 nm, as shown in Fig. 3. After the curing, the prepared epoxies exhibited no diffraction peak between the 2° and 10° (2θ) range for both the 5 and 10 wt% POP2000–2MA/LDH composites (Figs. 3c and 4d). Apparently, the layered platelet structure was exfoliated or expanded over 10 nm interlayer spacing beyond the XRD detection limit in both the cases. The XRD analyses indicated a fine dispersion of the LDH platelets in the epoxy matrices and the disappearance of clay ordered structure. Nevertheless, the wide-angle XRD may not reveal the result of exfoliation due to its detection limit. It relies on the TEM analysis for differentiating the further structure of exfoliated LDHs.

On the basis of DSC curing pattern, the curing conditions were established to be 120 °C for 1 h, 150 °C for 2 h, and 180 °C for 2 h.
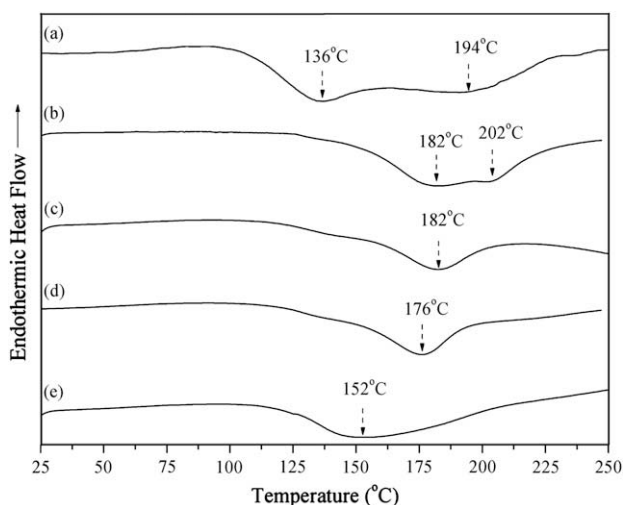

Fig. 3. X-ray diffraction patterns of (a) pristine LDH, (b) POP2000–2MA/LDH, (c) 5 wt% and (d) 10 wt% of POP2000–2MA/LDH cured epoxies, (e) POP400–3MA/LDH, (f) 5 wt% and (g) 10 wt% of POP400–3MA/LDH cured epoxies.

Under such a set of curing program, the epoxy nanomaterials were prepared and examined by TGA for their relative thermal degradation properties. As shown in Fig. 4, the weight loss analysis under the air flow demonstrated the patterns of the thermo-oxidative degradation of the organic components. With the identical heating pattern, the decomposition temperatures of 322, 361, and 335 °C for the 10 wt% weight loss and 358, 425, and 381 °C for the 50 wt% were observed for the epoxy composites cured by POP2000–2MA, POP2000–2MA/LDH, and POP400–3MA/LDH, respectively. The relative decomposition temperatures indicated that there is a stabilizing effect by the presence of the LDH clays. Especially for the POP2000–2MA/LDH cured epoxy, a significant increase in thermal stability was realized for epoxies cured by 5 wt% POP2000–2MA/LDH and 10 wt% POP400–3MA/LDH. Furthermore, although the LDH loading is double, the enhancement of the thermal stability in the 5 wt% POP2000–2MA/LDH epoxy was superior to that of 10 wt% POP400–3MA/LDH. This implies that the dispersion of LDH

Fig. 2. DSC thermograms of the epoxy self-polymerization in the presence of the initiators (a) POP2000–2MA, (b) POP2000–2MA sodium salt, and the POP2000–2MA/LDH with the LDH content of (c) 5 wt%, (d) 10 wt%, and (e) 15 wt%.
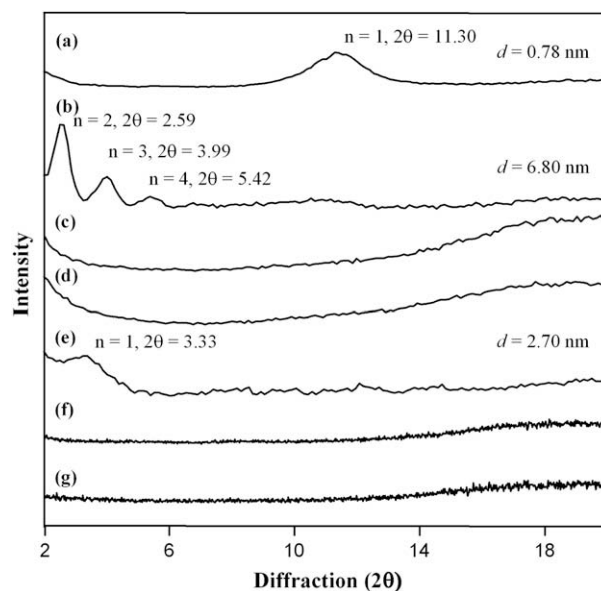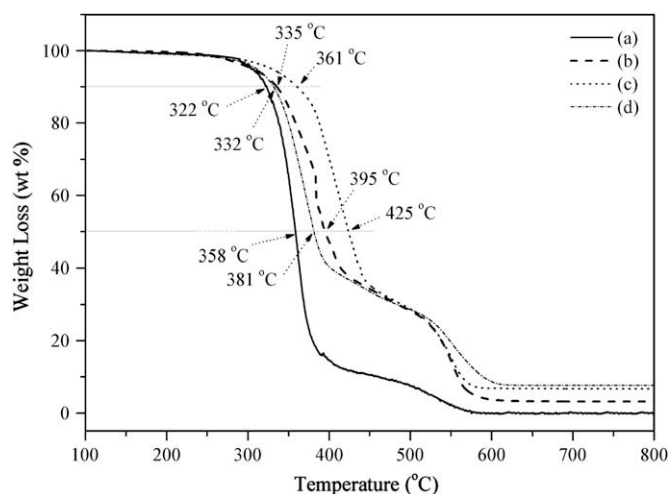

Fig. 4. TGA thermal degradation patterns of (a) POP2000–2MA cured epoxy, (b) 5 wt% and (c) 10 wt% POP2000–2MA/LDH cured epoxies, (d) 10 wt% POP400–3MA/LDH cured epoxy.
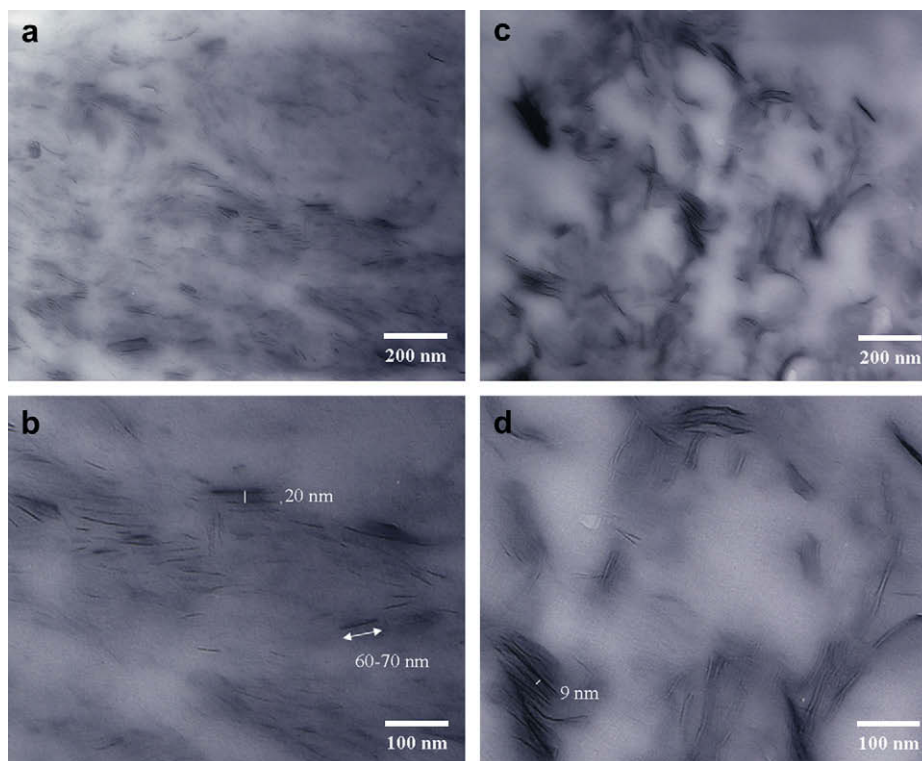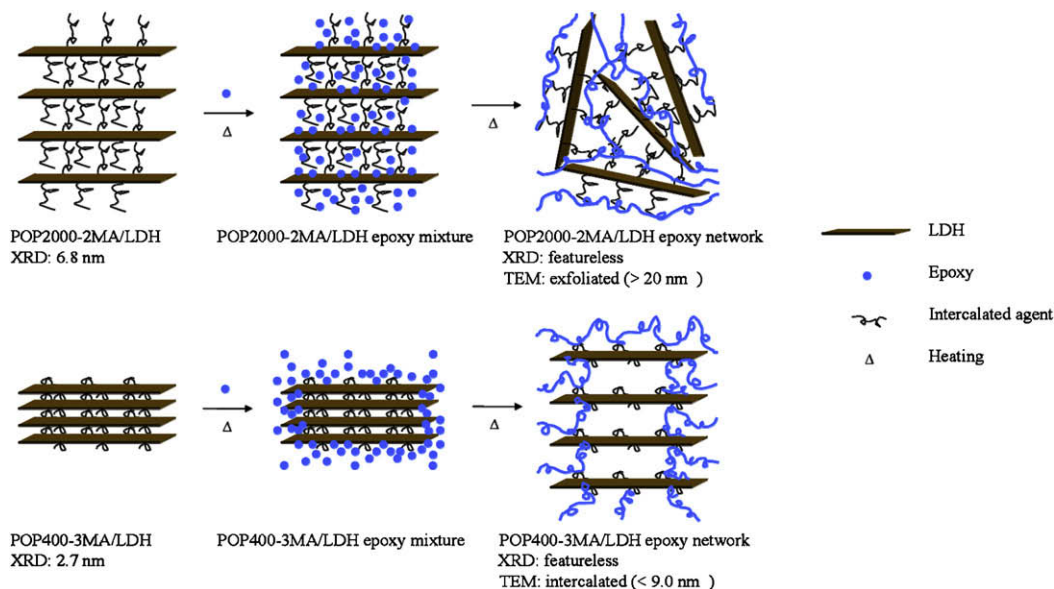
Fig. 5. TEM micrographs of (a) and (b) 10 wt% POP2000–2MA/LDH cured epoxy, (c) and (d) 10 wt% POP400–3MA/LDH cured epoxy.

and the exfoliation of their layered structure in the epoxy matrices are important for affecting the thermal properties.

3.3. Morphologies of POP–amido acid/LDH epoxy networks

By TEM, the distribution of silicate platelets in epoxy matrices was observable in the shape of interlayer lines from side view. The 10 wt% of POP2000–2MA/LDH cured in epoxy network was shown to have a fine platelet distribution. As demonstrated in Fig. 5a, most of the clay layered structures were exfoliated into flexible single layers (dark lines), with the dimension of the layered platelet at a maximal length of approximately 60–70 nm. In the magnified micrograph (Fig. 5b), the distance between two layers is

approximately 20 nm from the original 6.8 nm of the POP2000–2MA/LDH by XRD analysis. The overall distribution of the exfoliated platelets is homogeneous in the epoxy matrix. By comparison, POP400–3MA/LDH as the initiator for the epoxy self-cuing, the 10 wt% of layered LDH platelets had a dispersion of intercalated structures at average 10–15 layerly stacked structure (Fig. 5c). It appears that the layered d spacing is expanded from the original 2.7 to 7.5–9.0 nm interlayers (Fig. 5d). The complete exfoliation of POP400–3MA/LDH in epoxy is limited. The original widening of d spacing for the POP-intercalated LDH is essential for preparing the well dispersed nanocomposites of clay platelets in the epoxy matrices. It is envisioned that, during the epoxy curing process, the monomers enabled to migrate into clay galleries, subsequently

Scheme 1. Conceptual diagram of POP–amido acid/LDH initiated epoxy polymerization to form the intercalated or exfoliated networks.
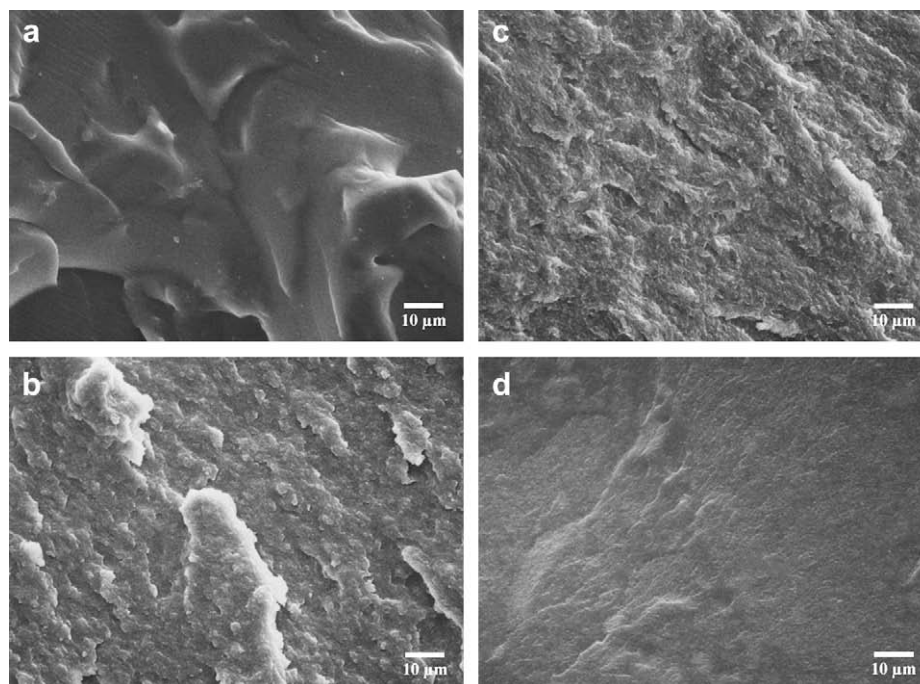
Fig. 6. SEM micrographs of the fractured surfaces of (a) POP2000–2MA cured epoxy, (b) 5 wt% and (c) 10 wt% POP2000–2MA/LDH cured epoxies, (d) 10 wt% POP400–3MA/LDH cured epoxy.

initiate the polymerization and exfoliate the LDH layered structure. In the POP2000 system (6.8 nm spacing), the electrostatic interaction force among the LDH layers was overcome to generate the exfoliated LDH in epoxies. In contrast, the low spacing (2.7 nm) POP400-intercalated clay had a relatively low content of organic embedment in the layered structure and failed to produce a totally exfoliated nanocomposite.

The intercalated or exfoliated LDH/epoxy matrices are conceptually illustrated in Scheme 1, for the layered structure expansion by the presence of DGEBA epoxy and its polymerization. The spatially expanded interlayer space in POP2000–2MA/LDH allows the accessibility of the DGEBA epoxy monomers for entering into the layered galleries and subsequent epoxy ring-opening polymerization. The LDH interlayer was further expanded and eventually exfoliated from the original 6.8 nm. On the contrary, the POP400–3MA/LDH had a narrower d spacing of 2.7 nm and lower organophilicity for the epoxy monomers. As a result, most of the epoxy monomers may just react to form polymers outside of the clay galleries. Although the ordinary laminar structure is expanded beyond the XRD detection limit, most of LDH still maintained the layered structures. As indicated by the TEM micrographs, the interlayer space was estimated to be 7.5–9.0 nm instead of an exfoliation.

SEM was used to examine the fractured surface of the epoxy matrices and the fractured surface roughness is relative to the mechanical properties [41,42]. Fig. 6a exhibits the fractured surface morphology of POP2000–2MA epoxy network as a smooth glassy surface. The morphologies of the POP–amido acid/LDH/epoxy networks showed different surface morphologies as indicated in Fig. 6b and c, for the 5 and 10 wt% POP2000–2MA/LDH epoxy networks, respectively. The fractured surface roughness is obviously increased in comparison with the POP2000–2MA cured epoxy, implying a high adhesive force under stress and the transfer of stress to the LDH. By comparison, the degree of roughness and irregularity of the surface rendered by the presence of 10 wt% of POP400–3MA/LDH in epoxy (Fig. 6d) were shown to have a relatively less roughness than that of the POP2000–2MA/LDH epoxy. These SEM observations on roughness are in good agreement with the exfoliated and intercalated implications. It was also correlated well with the TEM micrographs, in which the POP2000–2MA/LDH was superior to the POP400–3MA/LDH in terms of the fine dispersion of the individual platelets in epoxy matrices. The presence of LDH in epoxy had also affected the epoxy decomposition delay temperature. All the results indicated that the fine dispersion of the exfoliated platelets in the POP2000–2MA/LDH epoxy networks was superior to the intercalated platelets in the POP400–3MA/LDH

Table 1
Epoxy curing temperatures and thermal stabilities of the POP–amido acid/LDH cured epoxies

Initiator	LDH/POP–amido acid/epoxy (wt ratio)	T_p[a] (°C)	T_{d10}[b] (°C)	T_{d50}[b] (°C)	XRD
None	0/0/100	None	–	–	–
LDH	5/0/95	None	–	–	–
POP2000–2MA	0/25/75	136, 194	322	358	–
POP2000–2MA salt	0/25/75	182, 202	–	–	–
POP2000–2MA/LDH (6.8 nm)	5/20/75	182	332	395	XRD: featureless
	10/40/50	176	361	425	XRD: featureless (TEM: exfoliated)
POP400–3MA/LDH (2.7 nm)	5/6/89	–	325	360	XRD: featureless
	10/12/78	–	335	381	XRD: featureless (TEM: 7.5–9.0 nm)

–: Not measured.

[a] T_p: curing exothermic temperature determined by DSC scanning from 25 to 250 °C at a rate of 10 °C/min.

[b] T_d: relative thermal stability determined by TGA at 10 and 50 wt% weight loss.

epoxies. The possible correlation of the thermal properties for the epoxy materials from the POP and POP–LDH initiated epoxy self-polymerization is summarized in Table 1.

4. Conclusion

Two representative POP–amido acid intercalated LDH clays, POP2000–2MA/LDH (*d* spacing 6.8 nm) and POP400–3MA/LDH (*d* spacing 2.7 nm), are allowed to initiate the epoxy self-polymerization. The catalytic effect is established by examining DSC exothermic peaks at different LDH loadings, showing a shifting to lower temperature of 152 °C from 182 °C. Besides the fast curing, at 10 wt% of LDH loading, the self-cured epoxy demonstrated an enhanced thermal stability on the basis of TGA pattern, showing a significant difference between the POP–LDH initiators and the blank POP–amido acids. The LDH-exfoliated epoxy matrices are achieved by the spatially expanded POP2000–2MA/LDH system, but only partially exfoliation in POP400–3MA/LDH epoxy network (7.5–9.0 nm by TEM). The facile preparation of anionic LDH initiation of epoxy self-polymerization provides a new route for preparing clay-exfoliated nanocomposites.

Acknowledgments

References

[1] Giannelis EP. Adv Mater 1996;8:29–35.
[2] Utracki LA, Sepehr M, Boccaleri E. Polym Adv Technol 2007;18:1–37.
[3] Alexandre M, Dubois P. Mater Sci Eng 2000;28:1–63.
[4] Okada A, Usuki A. Mater Sci Eng C 1995;3:109–15.
[5] Okada A, Usuki A. Macromol Mater Eng 2006;291:1449–76.
[6] Ray SS, Okamoto M. Prog Polym Sci 2003;28:1539–641.
[7] LeBaron PC, Wang Z, Pinnavaia TJ. Appl Clay Sci 1999;15:11–29.
[8] Giannelis EP. Appl Organomet Chem 1998;12:675–80.
[9] Zanetti M, Lomakin S, Camino G. Macromol Mater Eng 2000;279:1–9.
[10] Ishida H, Campbell S, Blackwell J. Chem Mater 2000;12:1260–7.
[11] Bourbigot S, Devaux E, Flambard X. Polym Degrad Stab 2002;75:397–402.
[12] Ogata N, Kawakage S, Ogihara T. Polymer 1997;38:5115–8.
[13] Gilman JW, Jackson CL, Morgan AB, Harris RJ, Manias E, Giannelis EP, et al. Chem Mater 2000;12:1866–73.
[14] Zhu J, Morgan AB, Lamelas FJ, Wilkie CA. Chem Mater 2001;13:3774–80.
[15] Kawasumi M, Hasegawa N, Kato M, Usuki A, Okada A. Macromolecules 1997; 30:6333–8.
[16] Hasegawa N, Okamoto H, Kawasumi M, Usuki A. J Appl Polym Sci 1999; 74:3359–64.
[17] Hsueh HB, Chen CY. Polymer 2003;44:5275–83.
[18] Hsueh HB, Chen CY. Polymer 2003;44:1151–61.
[19] Triantafillidis CS, LeBaron PC, Pinnavaia TJ. Chem Mater 2002;14: 4088–95.
[20] Brown JM, Curliss D, Vaia RA. Chem Mater 2000;12:3376–84.
[21] Krishnamarooti R, Vaia RA, Giannelis EP. Chem Mater 1996;8:1728–34.
[22] Dusek K. Epoxy resins and composites. New York: Springer-Verlag; 1985.
[23] May CA. Epoxy resins, chemistry and technology. 2nd ed. New York: Marcel Dekker; 1988.
[24] Kobayashi M, Sanda F, Endo T. Macromolecules 2001;34:1134–6.
[25] Hino T, Endo T. Macromolecules 2004;37:1671–3.
[26] Pinnavaia TJ. Science 1983;220:365–71.
[27] Wang MS, Pinnavaia TJ. Chem Mater 1994;6:468–74.
[28] Lan T, Kaviratna PD, Pinnavaia TJ. J Phys Chem Solids 1996;57:1005–10.
[29] Hutchinson JM, Montserrat S, Roman F, Cortes P, Campos L. J Appl Polym Sci 2006;102:3751–63.
[30] Lin JJ, Cheng IJ, Chu CC. Polym J 2003;35:411–6.
[31] Chu CC, Lin JJ, Shiu CR, Kwan CC. Polym J 2005;37:239–45.
[32] Jan IN, Lee TM, Chiou KC, Lin JJ. Ind Eng Chem Res 2005;44:2086–90.
[33] Lin JJ, Cheng IJ, Wang R, Lee RJ. Macromolecules 2001;34:8832–4.
[34] Lin JJ, Cheng IJ, Chou CC. Macromol Rapid Commun 2003;24:492–5.
[35] Chou CC, Shieu FS, Lin JJ. Macromolecules 2003;36:2187–9.
[36] Lin JJ, Chang YC, Cheng IJ. Macromol Rapid Commun 2004;25:508–12.
[37] Lin JJ, Juang TY. Polymer 2004;45:7887–93.
[38] Leroux F. J Nanosci Nanotechnol 2006;6:303–15.
[39] Meyn M, Beneke K, Lagaly G. Inorg Chem 1990;29:5201–7.
[40] Lennon P, Espuche E, Sautereau H, Valo E. J Appl Polym Sci 2000;77: 857–65.
[41] Liu T, Phang IY, Shen L, Chow SY, Zhang WD. Macromolecules 2004;37: 7214–22.
[42] Wang K, Chen L, Wu J, Toh ML, He C, Yee AF. Macromolecules 2005;38: 788–800.